

Visual Field Prediction using Recurrent Neural Network - A Team Study on RNN

Aniruddha Anand Damle¹ Prakriti Biswas¹ Aditya Shrikant Kaduskar¹

¹Ira A. Fulton Schools of Engineering, Arizona State University

I. Abstract

In the past few years, one of the deep learning algorithms, the recurrent neural network (RNN), has shown an outstanding ability in sequence labeling and prediction tasks for sequential data. This paper focuses on building a reliable visual field prediction algorithm using RNN and evaluating its performance in comparison with the conventional pointwise ordinary linear regression (OLR) method. The performance of the RNN is compared with that of OLR by predicting the 6 visual fields in the test dataset.[7] The overall prediction performance of RNN was significantly better than OLR. The pointwise prediction error of the RNN was significantly smaller than that of the OLR in most areas known to be vulnerable to glaucomatous damage.[7] The RNN was also more robust and reliable regarding worsening in the visual field examination. In clinical practice, the RNN model can therefore assist in decision-making for further treatment of glaucoma.

II. What problem was solved? Why is it significant?

An RNN architecture was constructed in this study to receive a series of visual field evaluations and forecast future visual field damage. Glaucoma is the most common cause of blindness in the world.[1],[2]. The progressive loss of retinal ganglion cells (RGCs) and their axons characterize this chronic, irreversible optic neuropathy. Functional degradation of the visual field[2] as a result of structural abnormalities in ganglion cells has a significant impact on one's quality of life. Monitoring and identifying the progression of a visual field examination is a crucial activity in the prevention of vision loss in practice. The interpretation of visual field progression, on the other hand, is difficult. The visual field test, in particular, contains a high number of random errors and fluctuations, resulting in a low signal-to-noise ratio. Glaucoma patients experience more severe fluctuations than normal subjects.[3],[4]. The pattern of visual field progression over time varies greatly between patients.[5],[6]. Attempts to anticipate visual field status have been made in the past. Recent research has found that models with greater complexity produce better predictions.

III. How is raw data prepared and processed? Furthermore, what are the inputs and outputs of the deep networks?

Subjects who visited the glaucoma clinic at Pusan National University Hospital (South Korea) from 2005 to 2018 provided all training and test data. Both the training and test datasets contained subjects who had at least six consecutive visual field exams. The training dataset consisted of 1408 eyes of 841 subjects.[7] There was no diagnosis labeling on the training data. As a result, normal visual field data were included, as well as data from participants with glaucoma and other optic neuropathies; retinal disease and ocular media opacity (such as cataract) could potentially alter the visual field data. A total of 1408 [7] records from the training dataset were randomly split into training data + validation data at a ratio of 9:1[7]. To avoid overfitting, validation data were employed to assess the neural network's present fitness during training. Aside from the training dataset, a test dataset consisting of 281 eyeballs from 281 people was created. Between the training and test datasets, there was no patient overlap.

IV. Describe and introduce the deep network(s) used:

The final deep neural network architecture used in this study is shown in Fig. 1.

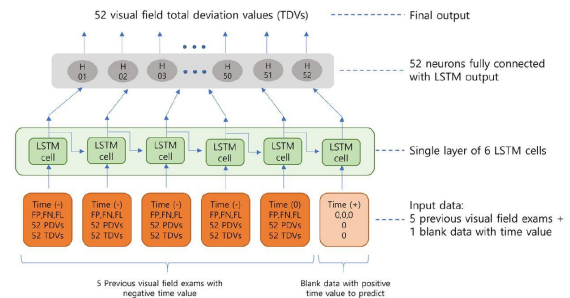


Fig. 1: Recurrent neural network architecture.[7]

Input data included 52 total deviation values (TDV), 52 pattern deviation values (PDV), reliability data (false-negative rate, false-positive rate, and total fixation loss rate), and temporal displacement value for a single layer of 6-LSTM cells. TDV, PDV, and time displacement values were normalized before being fed into the neural network by dividing them by 50, 50, and 10000, respectively.[7] The number of days since the most recent visual field examination

was used to calculate the time displacement value. The time displacement value with a negative sign indicates that the examination was completed in the past. One of the six visual field input data pieces had a particular format with positive time displacement (i.e., the point in the future that the user wanted to anticipate); all other data were set to 0. This particular input was utilized to provide information to the neural network about the date that the user wanted to anticipate. The LSTM layer is connected to the dense layer, which is a single fully connected layer with 52 neurons. A final visual field prediction is generated by these 52 neurons (1 neuron generates 1 visual field test point). Experimentation was used to come up with the final RNN architecture, which revealed that a single layer of LSTM with a single-layer fully linked network was the optimum neural network architecture.[7]

V. What algorithm was used to train the deep networks?

The model was trained with the Keras implementation of Adam[8], a first-order gradient-based stochastic optimization approach for stochastic objective functions based on adaptive estimations of lower-order moments for stochastic objective functions. RMS Propagation, which considers the exponential moving average, and Stochastic Gradient Descent with momentum are used by the Adam optimizer. When compared to a standard gradient descent algorithm, the exponential weighted average causes the procedure to converge faster to the minima. Adam is the best among the adaptive optimizers in most cases. Good with sparse data: the adaptive learning rate is perfect for this type of dataset. The method is easy to use, computationally efficient, takes little memory, is unaffected by gradient rescaling, and is well suited to issues involving huge amounts of data and/or parameters. The Adam optimizer is mathematically modeled by two equations:

$$\hat{m}_t = \frac{m_t}{1-\beta_1^t} \text{ and } \hat{v}_t = \frac{v_t}{1-\beta_2^t} [8]$$

m_t = Aggregate of gradients at time t

v_t = Sum of square of past gradients

β = Moving average parameter

Intuitively, this optimizer adapts the gradient descent method after each iteration. So the resulting general equation is:

$$w_{t+1} = w_t - \hat{m}_t \left(\frac{\alpha}{\sqrt{\hat{v}_t + \epsilon}} \right) [8]$$

The hyper-parameters have intuitive interpretations and don't necessitate a lot of tuning[8]. The learning rate (lr) was set to 1×10^{-3} at the start.

VI. What results were shown, and what performance measures were used to show the effectiveness of the deep network(s)?

$$RMSE = \sqrt{\sum_{n=1}^{52} \frac{(true\ TDV_n - predicted\ TDV_n)^2}{52}} [7]$$

$n = n^{th}$ test point of visual field exam

Using the equation below, MAE was determined for each test point of the visual field across all eyes.

$$MAE_n = \frac{\sum_{t=1}^{number\ of\ eyes} |true\ TDV_{t,n} - predicted\ TDV_{t,n}|}{number\ of\ eyes} [7]$$

$n = n^{th}$ test point of visual field exam, $i = i^{th}$ eye

$TDV_{t,n}$ = total deviation value of i^{th} eye and n^{th} test point

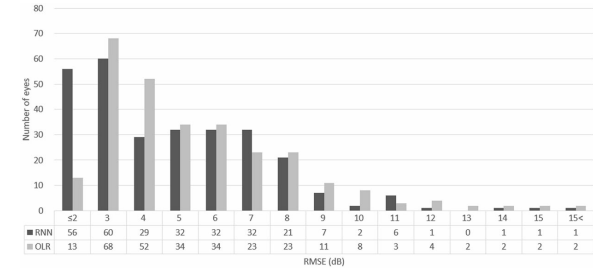


Fig. 2: The number of eyes binned by prediction error (RMSE). [7]

The RMSE or MAE of RNN and OLR were determined using those formulas. The authors employed a pairwise test for comparisons because the accuracy measures were paired (RNN, OLR). A significant difference in accuracy metrics (RMSE or MAE) between RNN and OLR was evaluated using a paired t-test or Wilcoxon's signed-rank test, depending on the normality of the data.

	Prediction error (RMSE, dB), mean \pm SD			P _{value}
	RNN	OLR	$\Delta_{OLR-RNN}$	
All patients	4.31 \pm 2.54	4.96 \pm 2.76	0.65	<0.001*
Normal	2.94 \pm 2.13	3.57 \pm 2.15	0.63	<0.001*
Glaucoma suspect	3.40 \pm 2.88	4.29 \pm 3.13	0.89	0.003*
Ocular hypertension	3.77 \pm 3.33	4.43 \pm 2.99	0.66	0.043*
Open angle glaucoma	5.29 \pm 2.00	5.81 \pm 2.44	0.52	0.004†
Normal tension glaucoma	4.62 \pm 2.15	5.23 \pm 2.46	0.61	0.008*
Angle closure glaucoma	5.27 \pm 2.52	5.09 \pm 3.38	-0.18	0.394†
Pseudoexfoliation glaucoma	3.95 \pm 2.04	5.80 \pm 0.85	1.85	0.285†
Others	3.08 \pm 2.80	4.61 \pm 3.57	1.53	0.009*

Table 1. Comparison of mean RMSE between RNN and OLR. OLR = ordinary linear regression; RMSE = root mean square error; RNN = recurrent neural network; SD = standard deviation. *Paired t-test. [†]Wilcoxon's signed rank test.[7]

To observe both parametric and nonparametric tests, the authors used Spearman's correlation analysis as well as simple linear regression analysis. They were used to look into trends in prediction errors based on factors like false-positive ratio, false-negative ratio, and

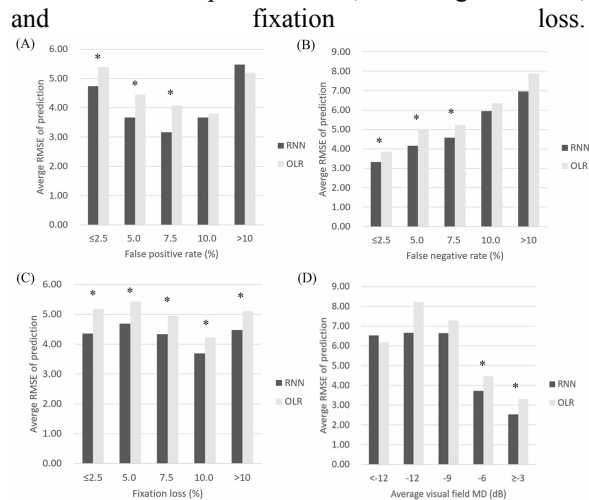


Fig. 3: Average prediction error (RMSE) binned by various factors. (A) RMSE vs. false positive rate (B) RMSE vs. false negative rate (C) RMSE vs. fixation loss (D) RMSE vs. visual field mean deviation (MD).[7]

The Shapiro-Wilk test was used to ensure that the data distribution was normal. SPSS (version 21.0 for Windows; SPSS, Chicago, IL, USA) was used in all statistical analyses, and a value of $P < 0.05$ was considered statistically significant. In general, RNN almost always showed lower prediction error than OLR. RMSE uniformly increased in both RNN and OLR as the false negative rate increased. False positive rate and visual field MD were considered to demonstrate a possible linear relationship with RMSE, but this trend was not uniform. RMSE vs. fixation loss was considered to demonstrate no obvious linear relationship. The symbol, asterisk (*), on top of the bar plot indicates the difference between RNN (dark gray bar) and OLR (light gray bar) is statistically significant. MD: mean deviation, OLR: ordinary linear regression, RMSE: root mean square error, RNN: recurrent neural network. The study concluded that building an RNN, a novel deep learning architecture, using a state-of-the-art LSTM algorithm results in significantly lower RMSE than OLR.

VII. Bibliography:

- [1] S. Resnikoff *et al.*, "Global data on visual impairment in the year 2002," *Bull. World Health Organ.*, vol. 82, no. 11, Nov. 2004 [Online]. Available: <https://pubmed.ncbi.nlm.nih.gov/15640920/>. [Accessed: 11-Feb-2022]
- [2] Y. C. Tham, X. Li, T. Y. Wong, H. A. Quigley, T. Aung, and C. Y. Cheng, "Global prevalence of glaucoma and projections of glaucoma burden through 2040: a systematic review and meta-analysis," *Ophthalmology*, vol. 121, no. 11, Nov. 2014, doi: 10.1016/j.ophtha.2014.05.013. [Online]. Available: <https://pubmed.ncbi.nlm.nih.gov/24974815/>. [Accessed: 11-Feb-2022]
- [3] "Sixth International Visual Field Symposium - Imaging and Perimetry .," *yumpu.com*. [Online]. Available: <https://www.yumpu.com/en/document/view/52055468/sixth-international-visual-field-symposium-imaging-and-perimetry->. [Accessed: 11-Feb-2022]
- [4] R. S. Brenton and W. A. Argus, "Fluctuations on the Humphrey and Octopus perimeters," *Invest. Ophthalmol. Vis. Sci.*, vol. 28, no. 5, pp. 767–771, May 1987 [Online]. Available: https://iovs.arvojournals.org/arvo/content_public/journal/iovs/933366/767.pdf. [Accessed: 11-Feb-2022]
- [5] D. B. Henson, S. Chaudry, P. H. Artes, E. B. Faragher, and A. Ansons, "Response variability in the visual field: comparison of optic neuritis, glaucoma, ocular hypertension, and normal eyes," *Invest. Ophthalmol. Vis. Sci.*, vol. 41, no. 2, Feb. 2000 [Online]. Available: <https://pubmed.ncbi.nlm.nih.gov/10670471/>. [Accessed: 11-Feb-2022]
- [6] P. Fogagnolo *et al.*, "Long-term perimetric fluctuation in patients with different stages of glaucoma," *Br. J. Ophthalmol.*, vol. 95, no. 2, Feb. 2011, doi: 10.1136/bjo.2010.182758. [Online]. Available: <https://pubmed.ncbi.nlm.nih.gov/20675728/>. [Accessed: 11-Feb-2022]
- [7] K. Park, J. Kim, and J. Lee, "Visual Field Prediction using Recurrent Neural Network," *Sci. Rep.*, vol. 9, no. 1, pp. 1–12, Jun. 2019, doi: 10.1038/s41598-019-44852-6. [Online]. Available: <https://www.nature.com/articles/s41598-019-44852-6>. [Accessed: 11-Feb-2022]
- [8] D. P. Kingma and J. Ba, "Adam: A Method for Stochastic Optimization," 22-Dec-2014 [Online]. Available: <http://arxiv.org/abs/1412.6980>. [Accessed: 11-Feb-2022]